

Shape Optimization of Homogeneous Electromagnets [★]

Dalibor Lukáš

SFB F013, University of Linz, Austria
Dept. of Applied Mathematics, VŠB-TU Ostrava, Czech Republic

Abstract. Magneto-optical effects are investigated among others for their application in storage media. Measurements of Kerr effect require magnetic field as homogeneous as possible. This is generated by so-called homogeneous electromagnets. The optimization aims at the optimal shape of the pole heads. The governing linear magnetostatic problem is approximated by the Finite Element Method (FEM) where quadratic triangular elements or edge elements are used in the 2-dimensional (2D) or 3-dimensional (3D) case, respectively. The solver is either a direct or multigrid Preconditioned Conjugate Gradient method (PCG), depending on the problem size. The Sequential Quadratic Programming (SQP) method with the BFGS update of Hessian matrix was used for the optimization. We computed an optimized 2D coarse design which was produced afterwards. The measurements show significant improvements of the homogeneity. We also computed an optimized 2D fine design by a hierarchical strategy, which is an iterative process where a coarse optimized shape is used as an initial design for the optimization on a finer grid. This approach seems to suit our class of problems very well. Finally, a coarse approximation of the 3D optimal shape was calculated.

1 Introduction

A number of applications needs homogeneous magnetic fields. They can be produced by electromagnets which impress such a field among the pole heads. These are called homogeneous electromagnets. In Fig. 1 there are two examples of them. In our case the homogeneous electromagnets are used for measurements of Kerr effect. The research of magneto-optical effects is interesting among others for the applications in magneto-optical storage media. This is investigated by the research team around prof. J. Pištorá at Department of Physics at VŠB - Technical University of Ostrava, see [2], with whom we closely cooperate.

This paper presents mathematical modeling and shape optimization of an electromagnet of a so-called Maltese Cross geometry. First, let's describe the physical problem. A sample of magneto-optical material is placed to the center of the Maltese Cross, see Fig. 2 (left). Rays coming to the center are polarized in the polarization plane by the magnetic field and then they

[★] This research has been supported by the Austrian Science Fund FWF within the SFB "Numerical and Symbolic Computing" under the grant SFB F013

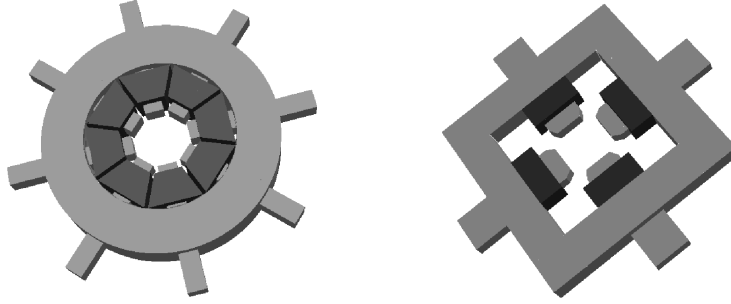


Fig. 1. Homogeneous electromagnets - geometries “O-ring” (left) and “Maltese Cross” (right)

reflect on the sample. The components of the reflected rays are measured. The field is to be as homogeneous as possible. By switching the sense of two currents we can polarize the rays in the orthogonal polarization plane as well. The device, see Fig. 2 (left), consists of a ferromagnetic yoke, 4 poles, and 4 windings. The shape of the pole heads influences the magnetic field in the plane significantly.

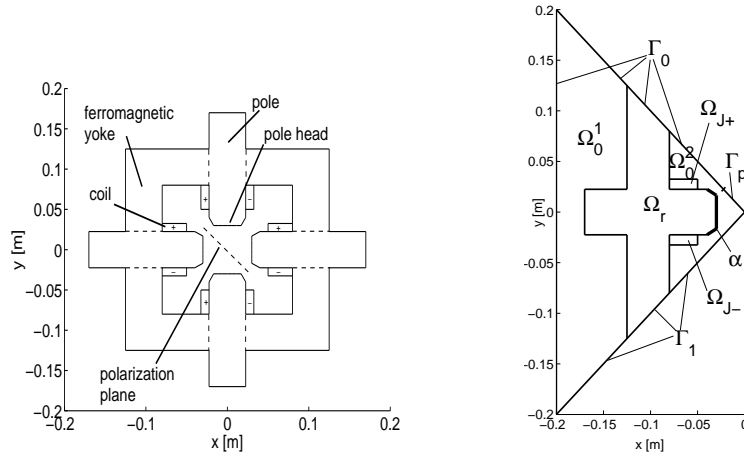


Fig. 2. Cross section of the Maltese Cross (left), computational domain Ω_{2D} (right)

2 Mathematical Model of the Maltese Cross

2.1 Linear Magnetostatic Problem

First we introduce Maxwell equations for 3D linear magnetostatics. Let $\overline{\Omega} := \cup_{i=1}^k \overline{\Omega}_i \subset \mathbf{R}^3$ be a material-wise decomposition where Ω is bounded and Ω_i are Lipschitz domains such that $\mu(x, y, z) = \mu_i$ denote domain-wise constant permeabilities of the appropriate materials. Further let \mathbf{B} denotes the

magnetic induction, \mathbf{H} is the magnetic strength density, and \mathbf{J} is the current density. Then the Maxwell equations formally read

$$\left. \begin{aligned} \mathbf{rot}(\mathbf{H}) &= \mathbf{J} \\ \mathbf{B} &= \mu\mathbf{H} \\ \mathbf{div}(\mathbf{B}) &= 0 \end{aligned} \right\} \text{ in } \Omega . \quad (1)$$

The corresponding mixed boundary conditions are

$$\left. \begin{aligned} \mathbf{B} \cdot \mathbf{n} &= 0 \quad \text{on } \Gamma_D , \\ \mathbf{H} \times \mathbf{n} &= \mathbf{0} \quad \text{on } \Gamma_N \end{aligned} \right\} \quad (2)$$

where $\partial\Omega = \overline{\Gamma_D} \cup \overline{\Gamma_N}$, $\Gamma_D \cap \Gamma_N = \emptyset$ and \mathbf{n} is the unit normal vector of $\partial\Omega$. Finally the interface conditions

$$\left. \begin{aligned} [\mathbf{B} \cdot \mathbf{n}]_{i,j} &= 0 , \\ [\mathbf{H} \times \mathbf{n}]_{i,j} &= \mathbf{0} \end{aligned} \right\} \quad (3)$$

hold where $[\cdot]_{i,j}$ denotes the jump on the interface $\Gamma_{i,j} := \overline{\Omega_i} \cap \overline{\Omega_j}$ and \mathbf{n} is the corresponding unit normal vector of $\Gamma_{i,j}$.

Now we introduce the magnetic vector potential \mathbf{A} as follows

$$\mathbf{rot}(\mathbf{A}) = \mathbf{B} , \quad \mathbf{div}(\mathbf{A}) = 0 . \quad (4)$$

We obtain the reduced 2-dimensional problem by looking at a typical cross section Ω_{2D} . There hold $\mathbf{J} = (0, 0, J(x, y))$, $\mathbf{B} = (B_x(x, y), B_y(x, y), 0)$, and the magnetic potential is uniquely given by

$$\mathbf{A} = (0, 0, u(x, y)) , \quad \mathbf{B} = \left(\frac{\partial u}{\partial y}, -\frac{\partial u}{\partial x}, 0 \right)$$

where u stands for the scalar potential.

We apply the 2D linear magnetostatics to the Maltese Cross problem. Since the magnetic field should be orthogonal to the polarization plane and, after switching the currents, to the orthogonal polarization plane as well, we prescribe the symmetric shapes of the pole heads. Therefore, the magnetic field is symmetric with respect to both of the polarization planes and we will deal only with a quarter of the original domain, see Fig. 2 (right). By using the scalar potential, the Maxwell setting of the 2D Maltese Cross problem formally reads as follows :

$$\left. \begin{aligned} -\mathbf{div} \left(\frac{1}{\mu} \nabla u \right) &= J \text{ in } \Omega_{2D} , \\ u &= 0 \text{ on } \Gamma_0 \cup \Gamma_p , \\ \frac{\partial u}{\partial \mathbf{n}} &= 0 \text{ on } \Gamma_1 \end{aligned} \right\} \quad (5)$$

with the interface conditions

$$\left. \begin{aligned} [\nabla u \times \mathbf{n}]_{i,j} &= 0 , \\ \left[\left(\frac{1}{\mu} \nabla u \cdot \mathbf{n} \right) \right]_{i,j} &= 0 . \end{aligned} \right\} \quad (6)$$

The parameters are $\mu = \begin{cases} \mu_0 & \text{in } \overline{\Omega} \setminus \overline{\Omega_r} \\ \mu_0 \cdot \mu_r & \text{in } \overline{\Omega_r} \end{cases}$, $\mu_0 = 4\pi \cdot 10^{-7} \text{ H.m}^{-1}$, $\mu_r = 5100$,

and $J = \begin{cases} 12.5 \text{ MA.m}^{-2} & \text{in } \Omega_{J_+} \\ 0 \text{ MA.m}^{-2} & \text{in } \Omega \setminus (\Omega_{J_+} \cup \Omega_{J_-}) \\ -12.5 \text{ MA.m}^{-2} & \text{in } \Omega_{J_-} \end{cases}$. Note that the ferromagnetic material is a kind of steel and J is given by the current $I = 6.3 \text{ A}$ and the wire diameter $d = 0.8 \text{ mm}$.

Finally, we set the weak formulation. Since the domains are Lipschitz, we can form the Hilbert ansatz space

$$V = \{v \in H^1(\Omega) \mid v = 0 \text{ on } \Gamma_0 \cup \Gamma_p\} . \quad (7)$$

Since $J \in L^2(\Omega_{2D})$ and $1/\mu \in L^\infty(\Omega_{2D})$ hold, the weak formulation of the 2D linear magnetostatic problem is well-defined and reads as follows :

$$\text{Find } u \in V : A(u, v) = b(v) \text{ for all } v \in V \quad (8)$$

where

$$A(u, v) := \int_{\Omega_{2D}} \frac{1}{\mu} \cdot \nabla u \cdot \nabla v \, dx , \quad b(v) := \int_{\Omega_{2D}} J \cdot v \, dx . \quad (9)$$

Note, that in the 3D case the boundary conditions are very similar and the weak formulation is built in $H(\mathbf{rot})$, see [1].

2.2 Shape Optimization Problem

Let Γ_p be the polarization line in Fig. 2 (right), in which inhomogeneities of the magnetic field are to be minimized. Let $\alpha \subset \partial\Omega_r$ be the graph of the shape of the pole head. Independently of the geometry of an electromagnet, we consider the following optimization problem :

$$\min_{\alpha \in \mathcal{F}} \varphi(\alpha) \quad (10)$$

under the constraints

$$\mathbf{B}_{\min}^{\text{avg}} \leq \|\mathbf{B}_\alpha^{\text{avg}}\| , \quad (11)$$

$$\alpha_l \leq \alpha \leq \alpha_u \quad (12)$$

where

$$\varphi(\alpha) := \frac{1}{\text{meas}(\Gamma_p) \cdot \|\mathbf{B}_\alpha^{\text{avg}}\|^2} \cdot \int_{\Gamma_p} \|\mathbf{B}_\alpha(\mathbf{r}) - \mathbf{B}_\alpha^{\text{avg}}\|^2 \, ds , \quad (13)$$

$$\mathbf{B}_\alpha^{\text{avg}} := \frac{1}{\text{meas}(\Gamma_p)} \cdot \int_{\Gamma_p} \mathbf{B}_\alpha(\mathbf{r}) \, ds , \quad (14)$$

$$\mathcal{F} := \{\alpha \subset \partial\Omega_r \mid \alpha \text{ is Lipschitz continuous and symmetric}\} , \quad (15)$$

and where $\alpha_l = -0.05 \text{ m}$, $\alpha_u = -0.03 \text{ m}$, and the typical average induction $\mathbf{B}_{\min}^{\text{avg}} = 0.25 \text{ T}$. This 2D formulation can be easily extended to 3D where α is a 2D function and Γ_p is the polarization plane.

3 Components of the Solver

The solver of the shape optimization problem uses the software of SFB F013. There are, namely, the finite element package FEPP [1], the mesh generator NETGEN [4], and the algebraic multigrid package PEBBLES [3] involved. This framework is mainly used to solve the state problem by the FEM method. In the 2D case we use quadratic triangular elements rather than linear to reach a better accuracy of the B-field. In the 3D case the edge elements [1] are used. The arising linear system is basically solved by the Conjugate Gradients method with a multigrid preconditioner. In the case when the number of unknowns is not large, a direct solver is applied.

The optimization method is based on the SQP method with the BFGS update of Hessian matrix. The optimization problem described in Sect. 2.2 is discretized and the design variables are x -coordinates of the nodes along the shape α which is interpolated linearly. The integrals in (13) and (14) are replaced by a quadrature formula of the 0th order. Derivatives are calculated by finite differences of the 3rd extrapolation order.

In shape optimization, once the shape has changed, the mesh is deformed. We use a simple strategy where nodes are displaced in the horizontal bar around the pole head only. The horizontal displacements are linearly dependent on the shape displacements as long as the node is far from the boundary α . For big displacements overlapping elements can appear. This happens within the line-search procedure and we simply exclude such designs α for which an element has flipped. Since only the feasible shapes are involved, the number of design variables is half the number of nodes along α such that the design is symmetric with respect to the x -axis. The shape α should also be Lipschitz continuous and, moreover, smooth enough because, otherwise, the linear magnetostatics is not valid and the shape is hardly producible. That's why, an additional regularity constraint on the maximal curvature of α has been implemented. Just for the purposes of an evaluating this constraint we interpolate the design nodes by cubic splines $\{\alpha_i\}$ and the curvature is calculated at each of the nodes along α . The constraint reads

$$-\frac{1}{\rho_{\min}} \leq \frac{\alpha_i''(x_i)}{\sqrt{[1 + (\alpha_i'(x_i))^2]^3}} \leq \frac{1}{\rho_{\min}} \quad \text{for all the design nodes } i \quad (16)$$

where $\rho_{\min} > 0$ is a minimal curvature radius. Note that the discretized shape itself remains piece-wise linear as we consider linear elements only.

In order to get fine enough results efficiently, a hierarchical optimization strategy has been implemented. We say that the classical approach is applied if only one discretized optimization problem is solved, i.e. the topology of the mesh doesn't change. By the hierarchical strategy we mean that several discretized optimization problems are solved sequentially such that they approximate the problem finer at higher levels and the optimized design is used as the initial one at the next level. There are a refinement and a prolongation

strategy involved. The refinement strategy deals with the refinement of the grid in order to get a better approximation of the cost functional and of the constraints. In our case we refine the discretization of Γ_p and use NETGEN for generation of the finer mesh. The prolongation strategy prolongs the optimized design to the finer level. It's done by using the interpolation of the shape by cubic splines such that the middle points of the splines are used at the finer level. A stopping criterion of the hierarchical strategy can be a convergence criterion of the cost function or a maximal number of levels. The hierarchical strategy is successful as far as the coarse optimized design approximates the fine one well.

4 Numerical Results

4.1 Comparisons of the 2D Coarse Optimized Design to Measurements

First, we present the 2D optimized design which we computed by the classical approach on a uniform mesh of the step size 2.5 mm and 25600 unknowns. The computational domain was the whole square. The initial design was the one in Fig. 2 (left). There were 5 design variables and the optimized design is shown in Fig. 3 (left). This was solved by MATLAB's Optimization Toolbox [5] and we reached the result in 5 iterations. Both of the constraints (11) and (12) were involved where $B_{\min}^{\text{avg}} = 0.18$ T. The derivatives were computed by the adjoint method of analytical sensitivity analysis.

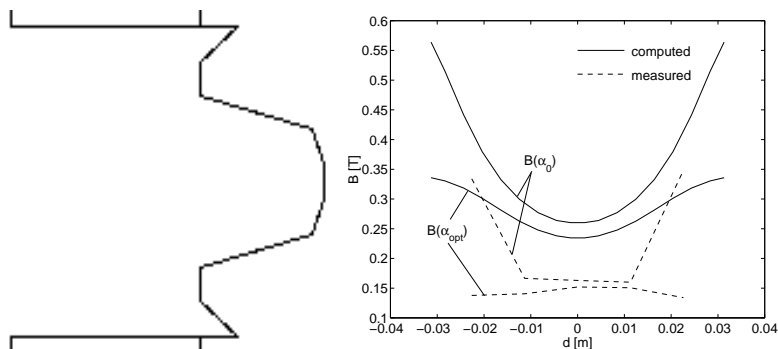


Fig. 3. 2D optimized pole head (left) and magnetic field comparisons (right)

This optimized design was produced and the magnetic field was measured at Department of Physics at VŠB-TU Ostrava. The measurements show significant improvements of the homogeneity. In Fig. 3 (right) there is drawn the magnetic induction along the polarization line Γ_p . The homogeneity of the optimized computed field has improved by the factor 10, and even much more

in the case of the measured field. Considering the state problem, we have observed that the nonlinear model would approximate the measurements well.

4.2 Hierarchical Optimization Strategy

We computed the 2D fine optimized design by the hierarchical optimization strategy. The constraint parameters were $B_{\min}^{\text{avg}} = 0.25 \text{ T}$ and the minimal curvature radius $\rho_{\min} = 1 \text{ cm}$. The computation proceeded at 3 levels with 3, 6, and 11 design variables, respectively. Properties of the computation are presented in Fig. 4. We can see that there is no need of a remeshing. The last column shows improvements of the cost function at each of the levels. Even if the discretized optimization problem at different levels is different, we can observe some convergence of the cost function $\varphi_l(\alpha_l)$. Finally, note that the classical approach takes 10 mesh regenerations when applied for the 11 design variables. Thus, the hierarchical approach is more efficient for our optimization problems.

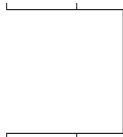
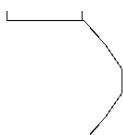
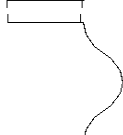
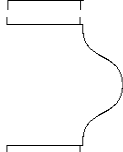
level l	optimized designs α_l	# of des. variables	# of unknowns	# of remeshs.	$\varphi_l(\alpha_{l-1})$ ↓ $\varphi_l(\alpha_l)$
0 (init.)		3	482		0.1068
1		3	482	0	0.1068 ↓ 0.0162
2		6	1469	0	0.0166 ↓ 0.0140
3		11	3331	0	0.0145 ↓ 0.0135

Fig. 4. Hierarchical optimization strategy

4.3 Optimized 3D Shape

At the end we present a result computed in 3D. As far as the state problem is considered, we use edge elements and the number of unknowns is 2516.

Considering the optimization, there are 4 design variables, $B_{\min}^{\text{avg}} = 0.2 \text{ T}$. We used the classical approach with 2 mesh regenerations. The optimized design is in Fig. 5. From the first glance it seems that the 2D optimized design is a good approximation of the 3D one.

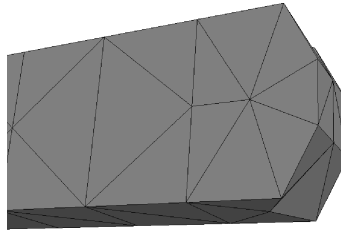


Fig. 5. Optimized 3D shape

5 Conclusions

We formulated a setting of the Maltese Cross problem in 2D. The 2D coarse optimized pole head was produced and the measurements have shown significant improvements of the homogeneity. We have found the hierarchical optimization strategy efficient for our problems. At last, the optimized coarse 3D result is quite similar to the 2D one.

One of the most important tasks for further work is an implementation of the direct and the adjoint technique of analytical sensitivity analysis. We will also investigate the hierarchical strategy more and apply it to the 3D case. We expect that with those properties the optimization solver will suit the problems of optimal shaping of homogeneous electromagnets very well. Finally, we will compute nonlinear problems and test the method for other geometries of homogeneous electromagnets.

References

1. M. Kuhn, U. Langer, and J. Schöberl. Scientific computing tools for 3d magnetic field problems. *The Mathematics of Finite Elements and Applications*, pages 239–259, 2000.
2. J. Pištora, K. Postava, and R. Šebesta. Optical guided modes in sandwiches with ultrathin metallic films. *Journal of Magnetism and Magnetic Materials*, 198–199:683–685, 1999.
3. S. Reitzinger. PEBBLES – user’s guide. SFB ”Numerical and Symbolic Scientific Computing”, <http://www.sfb013.uni-linz.ac.at>.
4. J. Schöberl. NETGEN - An advancing front 2D/3D-mesh generator based on abstract rules. *Comput. Visual. Sci.*, pages 41–52, 1997.
5. The MathWorks, Inc. *MATLAB Optimization Toolbox User Manual*, 1993.